# Global transition-zone topography and elastic properties from normal-mode tomography

**Rûna van Tent**[1], Lars Gebraad[2], Andreas Fichtner[2], Jeannot Trampert[1], Arwen Deuss[1]

[1]Department of Earth Sciences, Utrecht University, Utrecht, The Netherlands, [2]Department of Earth Sciences, ETH Zürich, Zürich, Switzerland

## 1. Introduction

The transition-zone discontinuities at 410 and 660 km depth are characterized by phase transitions in olivine. The depths of these phase transitions are temperature dependent, governed by their Clapeyron slopes (dP/dT), resulting in a thin transition zone in warm regions and a thick transition zone in cold regions (**Fig. 1**). In the absence of variations in chemical composition and water content, we then expect to see an anticorrelation between the discontinuity depth and velocity or density variations at the 410 discontinuity, while positive correlations are expected at the 660 discontinuity.

We present new global models of transition-zone topography, seismic velocities and density made using normal-mode data and discuss whether temperature variations can explain these models.

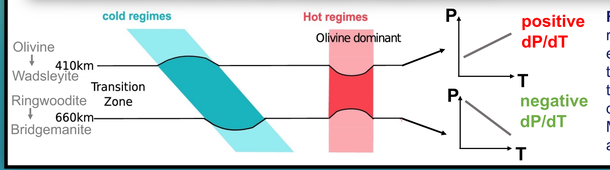


**Figure 1 |** Schematic representation of the effect of temperature on transition-zone topography controlled by olivine phase transitions. Modified from Jenkins et al. (2016).

## 2. Data & inversion method

**Normal modes** are whole Earth oscillations, i.e. standing waves along the surface and radius of the Earth, that appear as distinct peaks in the frequency spectrum of a seismogram (**Fig. 2**). We use measurements of spheroidal modes ($_nS_l$) from Deuss et al. (2013) and Koelemeijer et al. (2013).

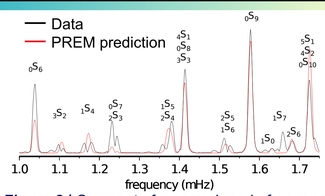


**Figure 2 |** Segment of a normal-mode frequency spectrum, including the prediction for PREM.

**Normal-mode splitting functions,** our data, describe the local frequency changes of a mode caused by 3-D velocity and density structure and discontinuity topography. As an example, **Fig. 3** shows measurements for modes $_0S_{21}$ (with upper-mantle sensitivity) and $_0S_5$ (with lower-mantle sensitivity), including the linear sensitivity kernels for $V_s$, $V_p$ and density.

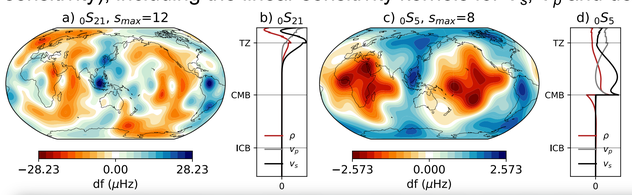


**Figure 3 |** Examples of splitting functions (a, c) and sensitivity kernels (b, d) for modes $_0S_{21}$ and $_0S_5$.

Since normal modes are directly sensitive to $V_s$, $V_p$, density and topography variations, we can create joint models of these parameters that can be readily compared to one another, without requiring velocity corrections.

### Inversion method

We solve the linear inverse problem using the Hamiltonian Monte Carlo (HMC) method (e.g. Neal 2011, Betancourt 2018). We use Gaussian priors over the data and the model parameters and therefore sample the least-squares posterior distributions. We parameterize our model using 7 B-splines (**Fig. 4**).

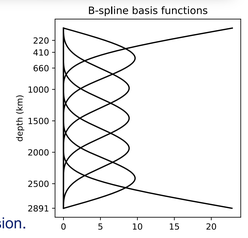


**Figure 4 |** B-spline parameterization used in our inversion.

## 3. Transition-zone models

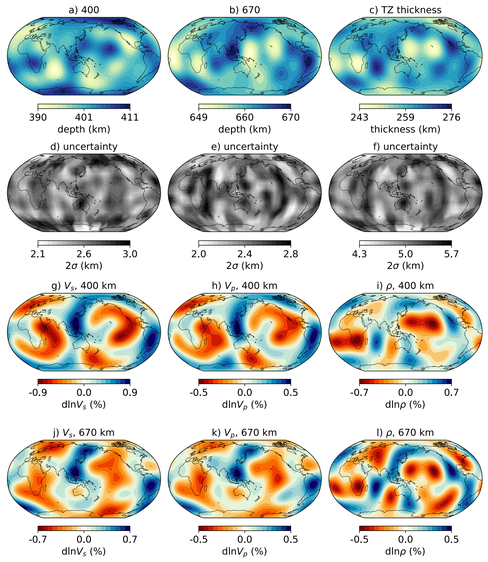


**Figure 5 |** Mean models of transition-zone topography and thickness (a-c) with corresponding uncertainties (d-f), as well as mean models of $V_s$, $V_p$ and density ($\rho$) at the discontinuity depths (g-l).

### 410-km discontinuity

- The regions under Hawaii and southern Africa, where the 410 is depressed and the transition zone is thin, correspond to low density but slightly increased seismic velocities.

### 660-km discontinuity

- The ring around the Pacific ocean, where the transition-zone is thick and where subducted slabs are expected to be present, shows a mostly depressed 660 with high seismic velocities and high density.
- The regions where the 660 is uplifted correspond to low seismic velocities and low density.

## 4. Topography correlations

We compare the correlations between topography and the $V_s$ and density models at the discontinuity depths (400 km and 670 km in PREM) with the expected correlations for changes in temperature **(Fig. 6).**

- For the 410-km discontinuity, $V_s$ and topography are (positively) correlated, which cannot be explained by temperature variations
- Density is a better indicator of transition-zone thickness than $V_s$
- Topography variations on the 410 and the 660 are uncorrelated

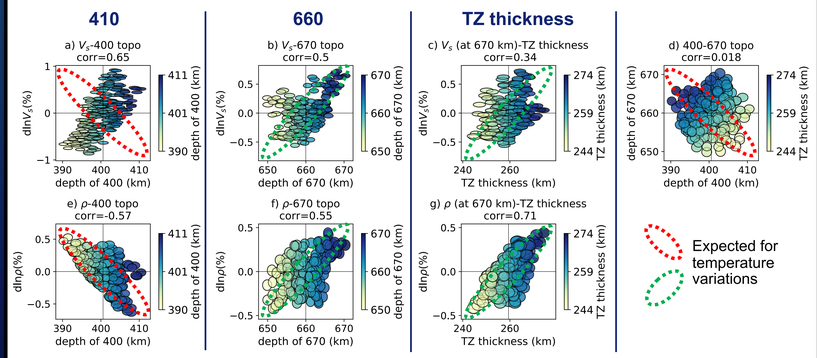


**Figure 6 |** Model correlations between the depths of the transition zone discontinuities and $V_s$ and density ($\rho$). The expected correlations for model variations caused by changes in temperature are also shown (schematically).

## 5. Comparison to other models

We also compare (**Fig. 7**) our normal-mode topography models (**a,e,i**) to three models filtered at the same spherical-harmonic degrees (s=2,4,6): a model where we add surface-wave phase velocities as data to our inversion (**b,f,j**), the surface-wave model (**c,g,k**) from Meier et al. (2009) and the SS precursor model (**d,h,l**) from Waszek et al. (2021).

For the 410-km discontinuity, normal-mode mode topography models are more similar to surface-wave models. For the 660, the most prominent depressions in topography are present in all models, but our model corresponds best to the body-wave model.

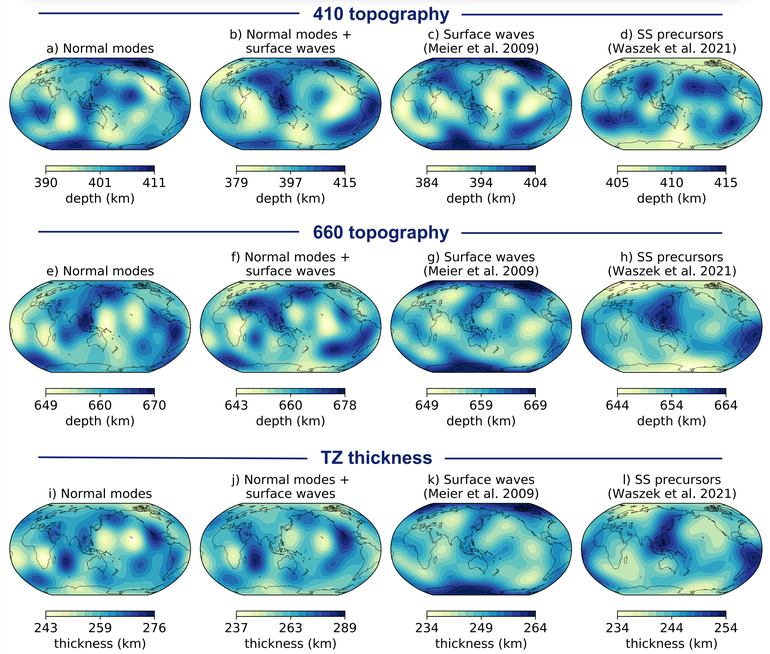


**Figure 7 |** Comparison of different transition-zone topography models at spherical-harmonic degrees s=2,4,6.

## 6. Conclusions & outlook

- Using recent normal-mode measurements we are able to resolve transition-zone topography without requiring constraints from other data types
- Density is a better indicator of transition-zone thickness than $V_s$
- Other variations than temperature (e.g. in composition or water content) are required to explain the correlations between our different model parameters

### Outlook

- Thermochemical interpretation
- Compare our transition-zone models to attenuation models (**Fig. 8**)
- Improve joint inversion with normal modes and surface waves

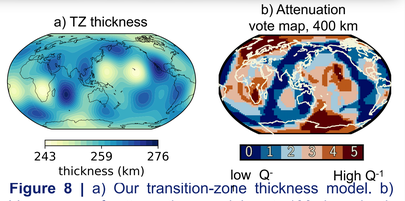


**Figure 8 |** a) Our transition-zone thickness model. b) Vote map of attenuation models at 400 km depth (s=2,4,6), see also Sujania Talavera Soza's poster.